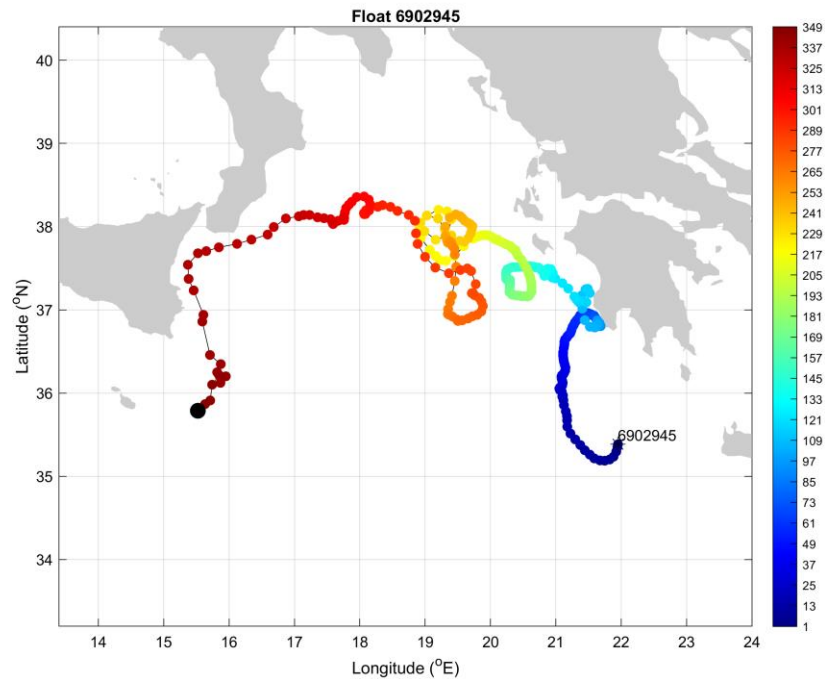# Delayed Mode Quality Control of Argo float WMO 6902945

Antonella Gallo

ORCID ID: 0000-0002-8836-1550

National Institute of Oceanography and Applied Geophysics - OGS
Borgo Grotta Gigante 42/C - 34010 - Sgonico (TS) – Italy
05/08/2022

Contents

1 Introduction

This report includes the delayed mode analysis performed for float 6902945. It was deployed in Mediterranean Sea (Ionian sub basin) in September 2019 and performed 349 cycles. It is still active. Before the analysis, real-time QC flags were visually inspected. The list of flags applied is QC=1 to all cycles. Plots of temperature and salinity time series and plots of temperature, salinity and density plotted against the nearby historical CTD profiles was generated. This visual analysis can help in detecting sensor salinity anomalies and spikes.

The reference dataset used is composed of the following CTD and Argo historical datasets:

CTD:
- CMEMS: INSITU_GLO_TS_REP_OBSERVATIONS_013_001_b
- Coriolis: CTD_for_DMQC_2021V01
- Historical CTD profiles provided through personal contact

Argo:
- ARGO_for_DMQC_2020V03

Float 6902945 is the Arvor float where the pressure sensor is auto corrected and no adjustment is required. The OWC was run to estimate a salinity offset and a salinity drift (Cabanes et al., 2016).

2 Quality Check of Argo Float Data

2.1 Verification of Real-time Mode QC flags

The list of flags applied to the float in real-time mode is as follows.

Cycle number:
1-349 PSAL QC=1

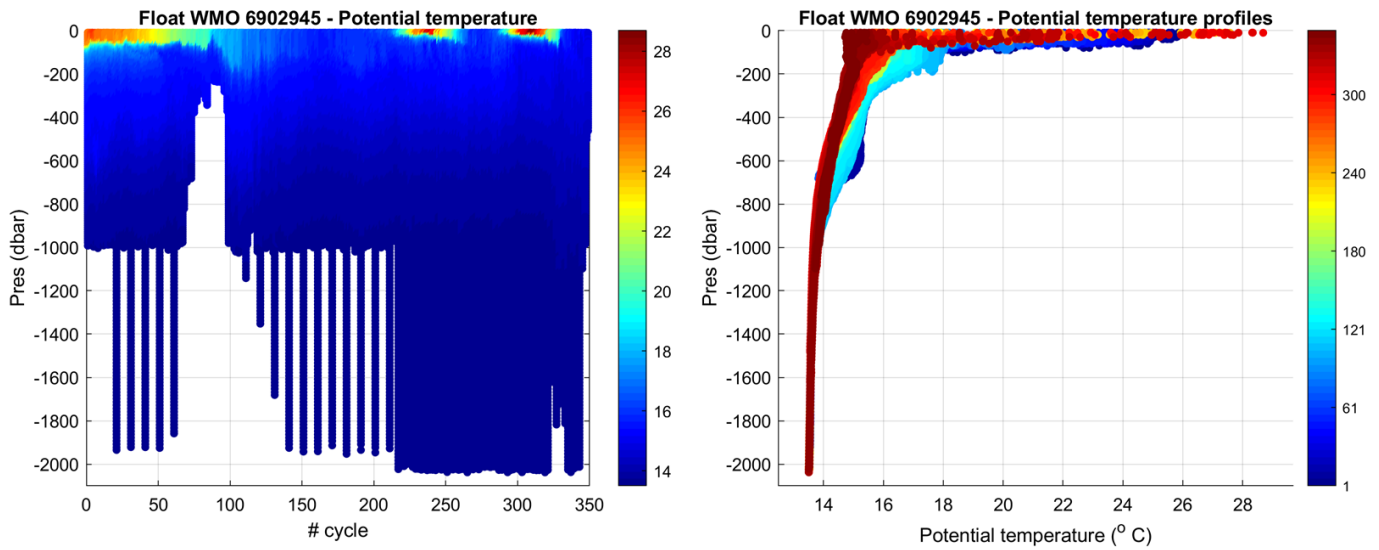## 2.2   Time Series of Argo Float Temperature and Salinity

Figure 1: Float 6902945. Time series of Argo float potential temperature (°C) on the left, and potential temperature profiles color-coded per cycle number on the right.
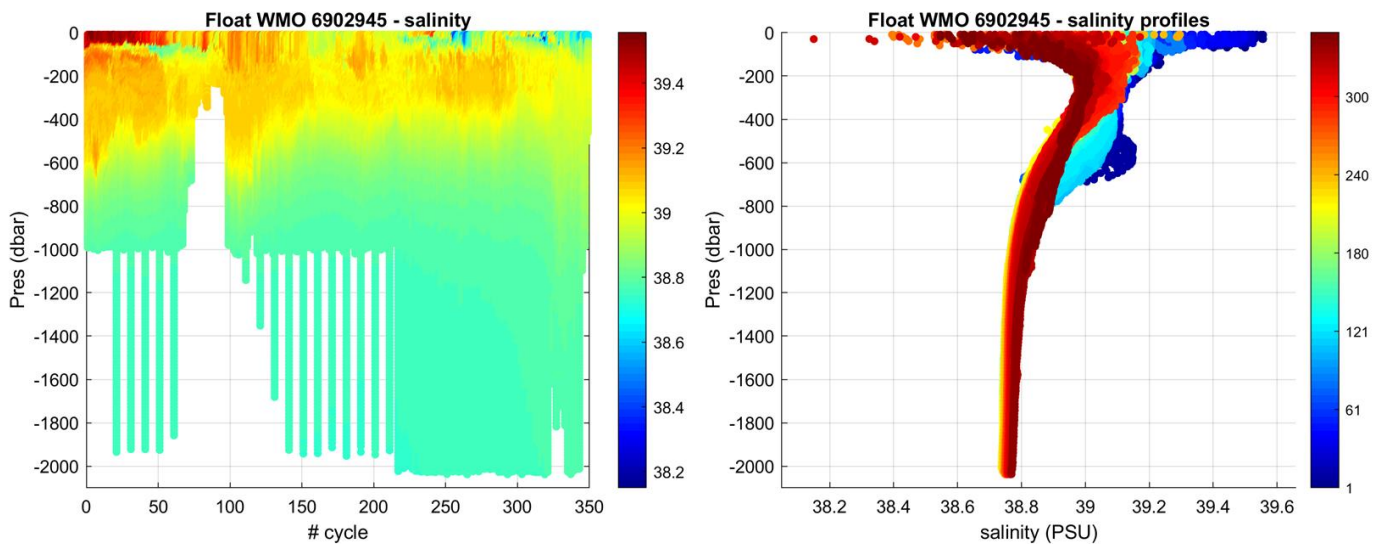

Figure 2: Float 6902945. Time series of Argo float potential salinity (PSS-78) on the left, and salinity profiles color-coded per cycle number on the right.

Before running the Owens and Wong method, referred to as OW hereafter, the theta-salinity (θ-S) diagram of the float is analyzed (Figure 3) and in particular the area where the θ-S relationship is the tightest (Figure 4). A significant salinity drift is observed.
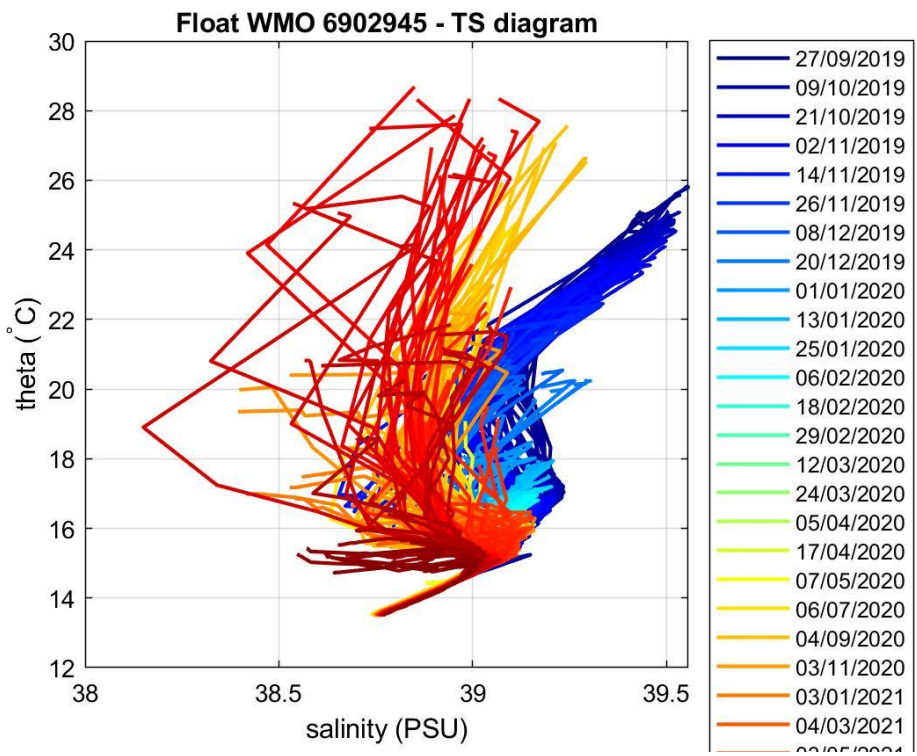
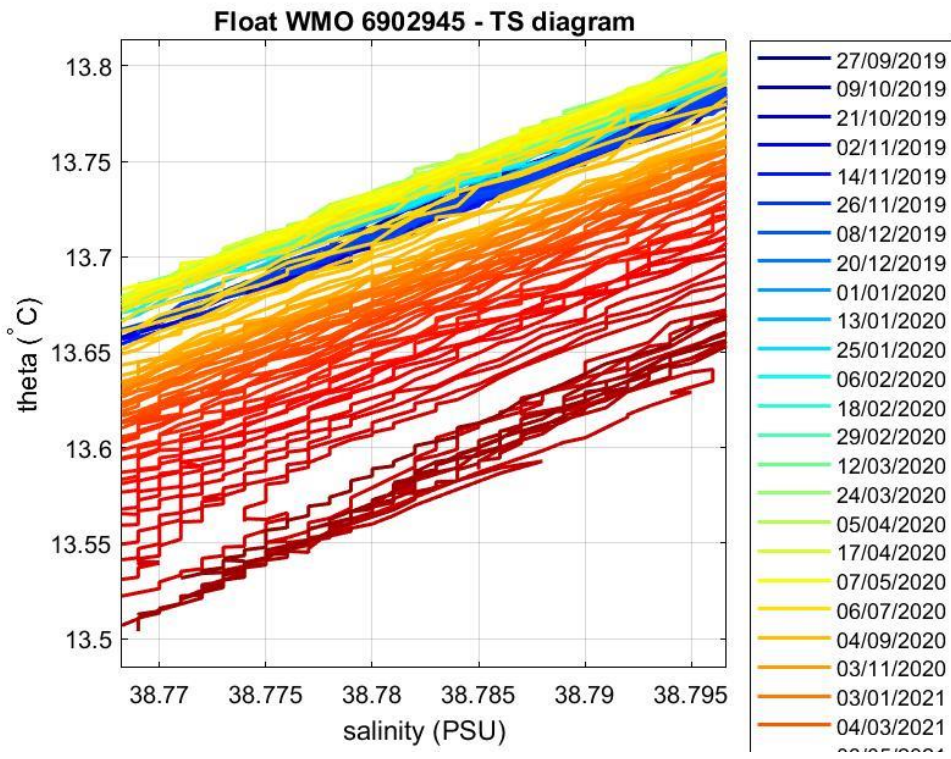**Figure 3:** Float 6902945. θ-S diagram color-coded per cycle number.

Figure 4: Float 6902945. Area of the θ-S diagram (color-coded per cycle number) where the θ-S relationship is more uniform.

2.3 Comparison Between Argo Float and Climatology

Three salinity float profiles are selected to perform a comparison (in time and space) with the historical data. In figure 5, 6 and 7 each selected profile is compared with all reference data used in this analysis. The salinity float profile is depicted in black while other colors represent the salinity reference profiles. The red color means that the historical data are more recent with respect to the float ones, while magenta states that the float data are more recent than the historical ones (the maximal difference is 9 years). A time difference between 3 and 6, 6 and 9 and larger than 9 years is depicted in green, cyan and blue, respectively.
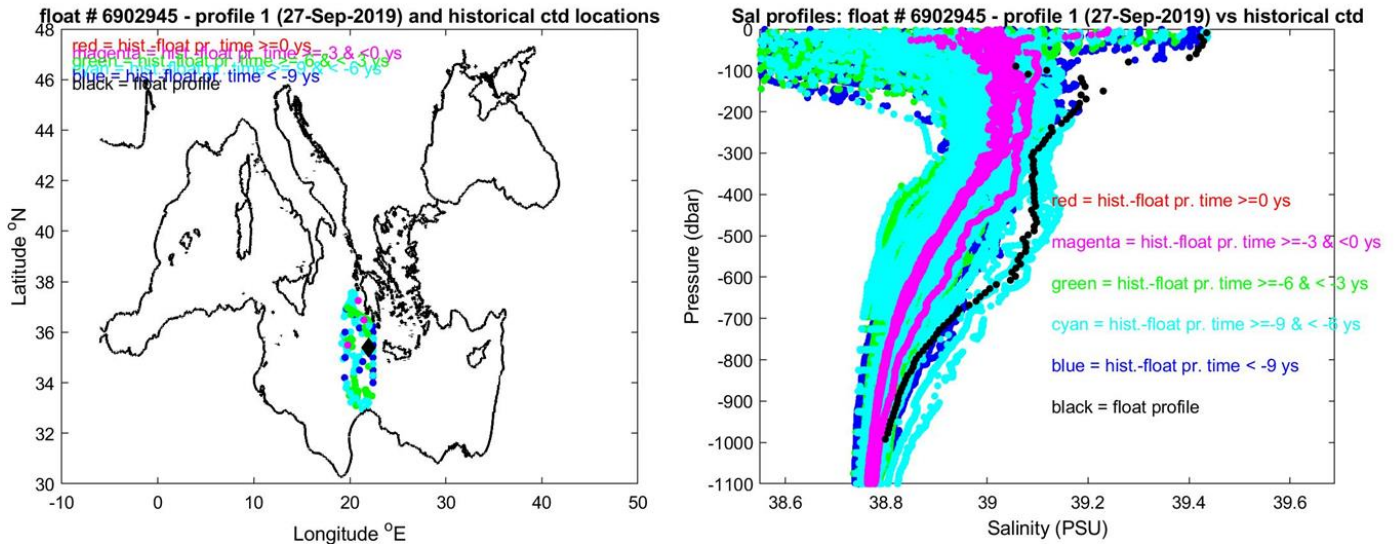

Figure 5: Float 6902945. Locations of the salinity float profile number 1 and historical CTD data (right panel) and the respective salinity profiles (left panel).
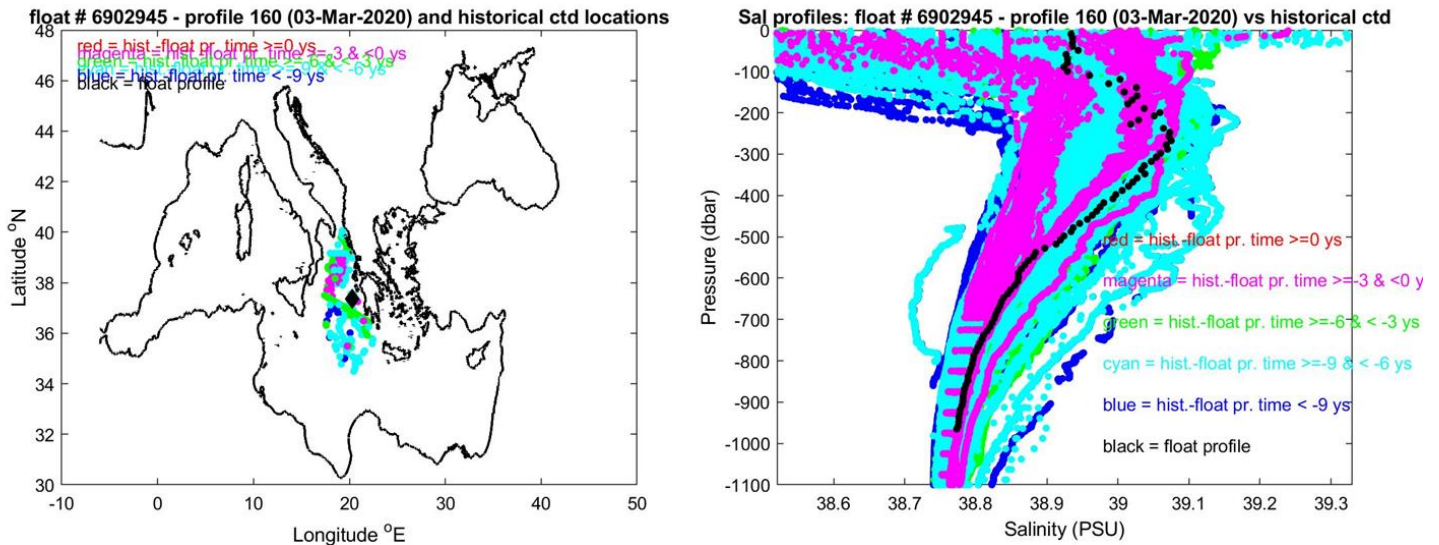

Figure 6: Float 6902945. Locations of the salinity float profile number 160 and historical CTD data (right panel) and the respective salinity profiles (left panel).
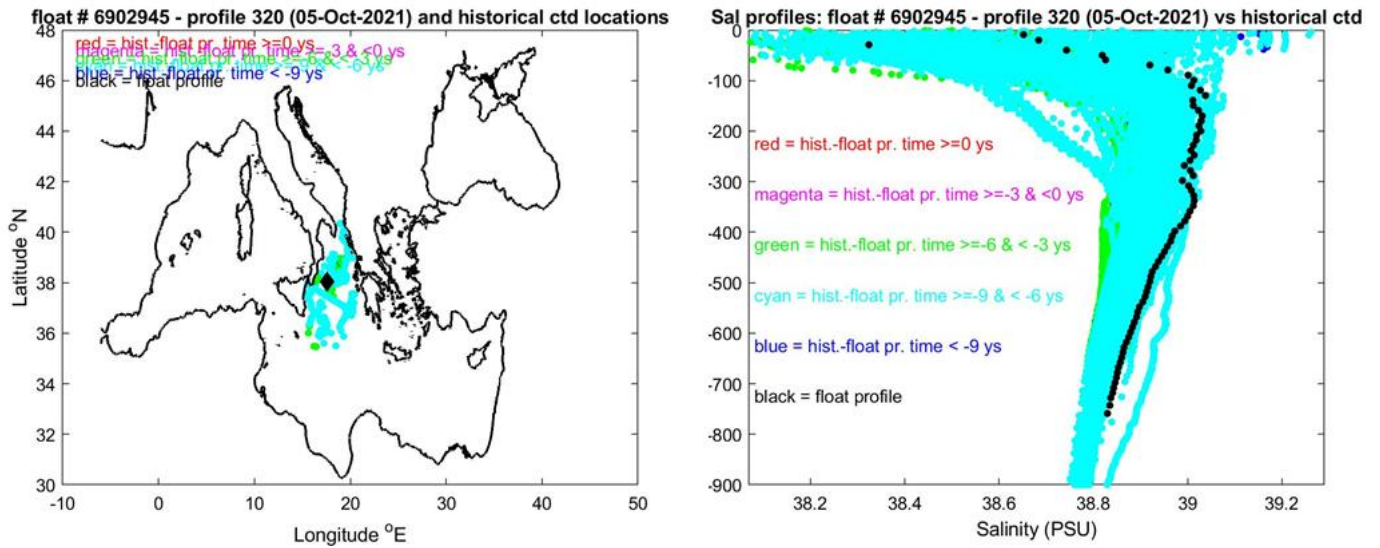
Figure 7: Float 6902945. Locations of the salinity float profile number 320 and historical CTD data (right panel) and the respective salinity profiles (left panel).

The comparison of these 3 selected salinity float profiles with the closest (in space and time) salinity reference profile in shown in Figures from 8 to 10. The agreement between the selected float salinity profiles and the historical salinity profiles is quite good in the intermediate and deeper layers, where the water column is more stable, for cycles 1 and 169.The comparison is not good for cycle 320.
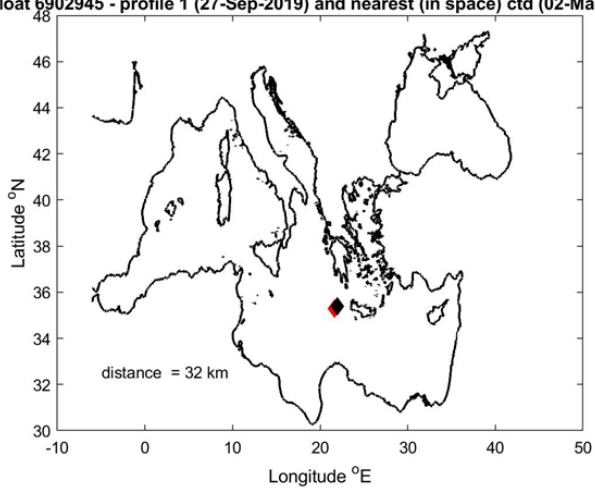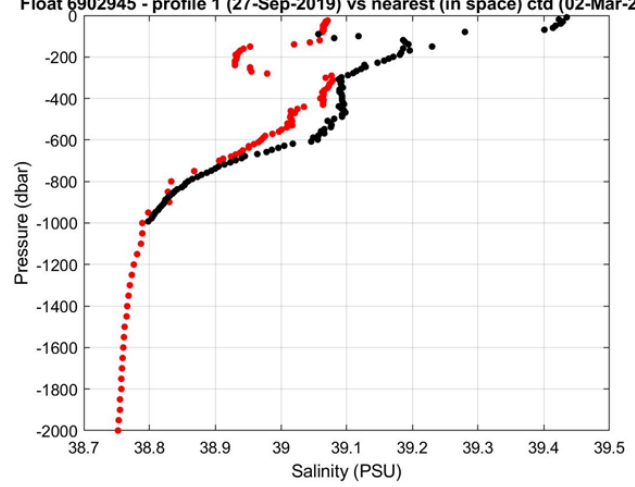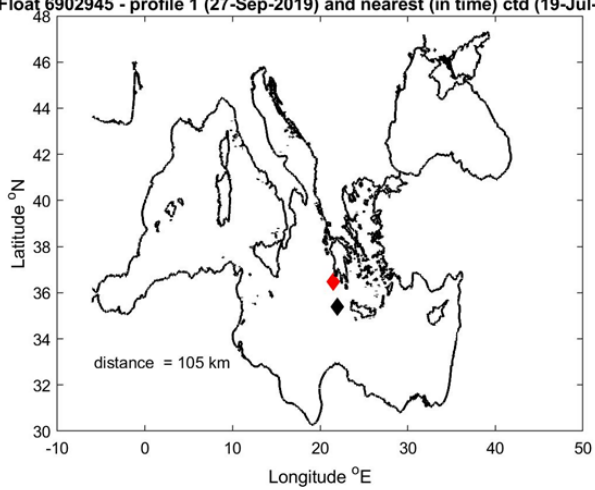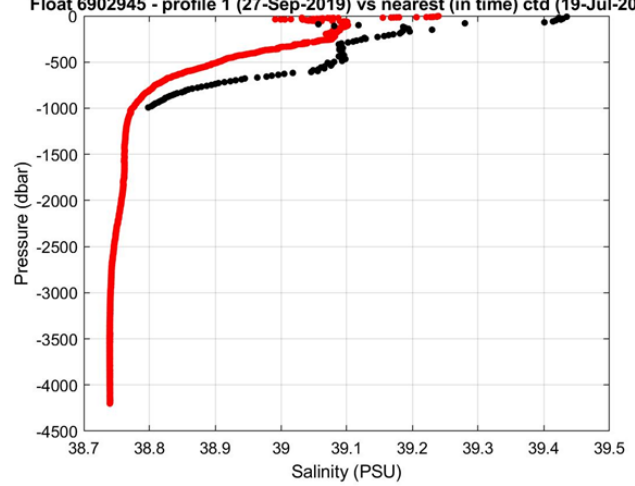
Figure 8: Float 6902945. The salinity float profile number 1 (black dots) are compared to the nearest in space (top) and in time (bottom) reference profile (red dots). The locations of the two profiles and their distance is given in the left panel.
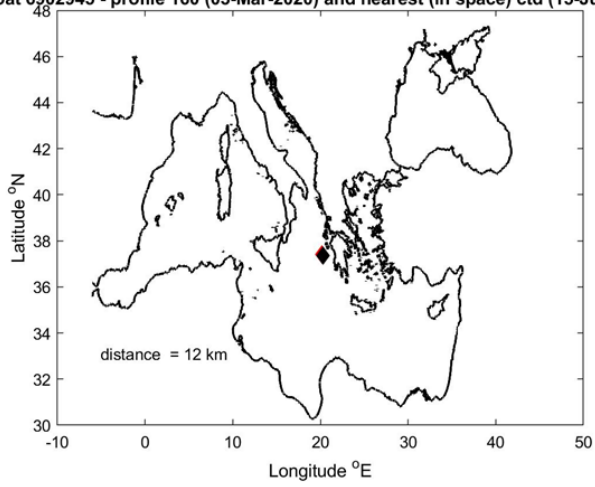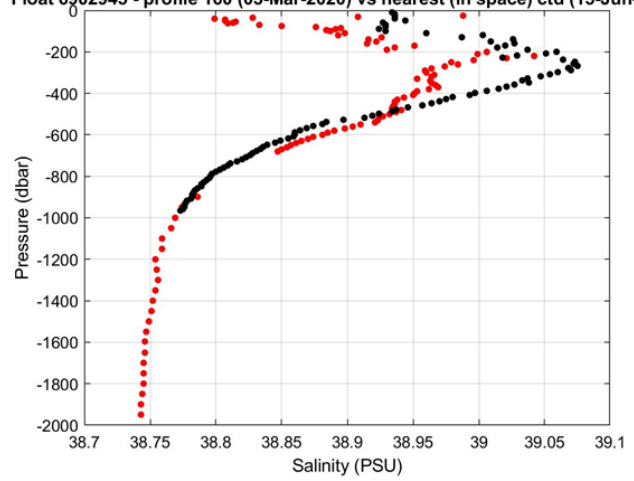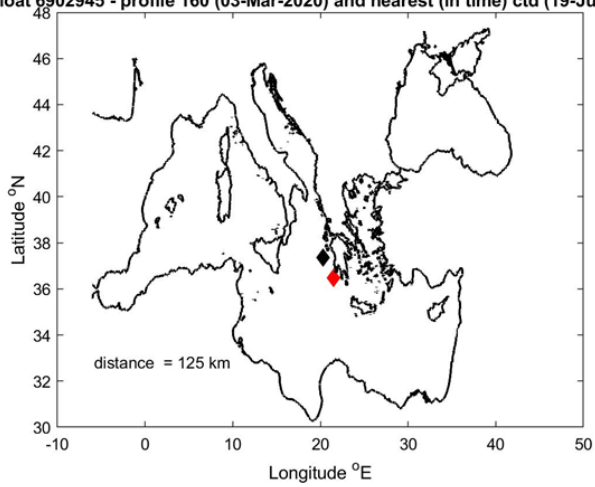
Figure 9: Float 6902945. The salinity float profile number 160 (black dots) are compared to the nearest in space (top) and in time (bottom) reference profile (red dots). The locations of the two profiles and their distance is given in the left panel.

Figure 10: Float 6902945. The salinity float profile number 320 (black dots) are compared to the nearest in space (top) and in time (botton) reference profile (red dots). The locations of the two profiles and their distance is given in the left panel.
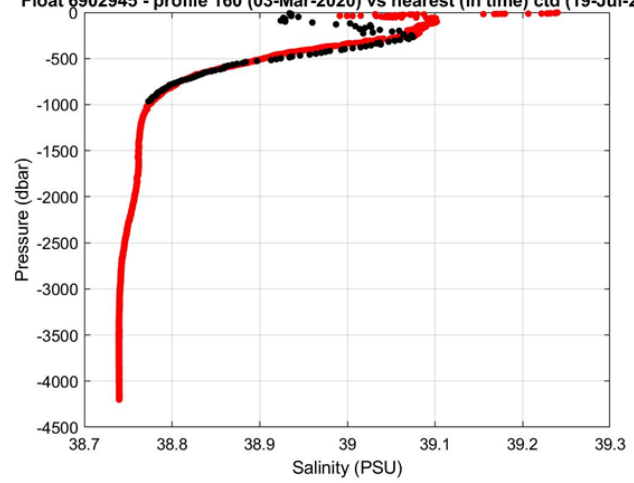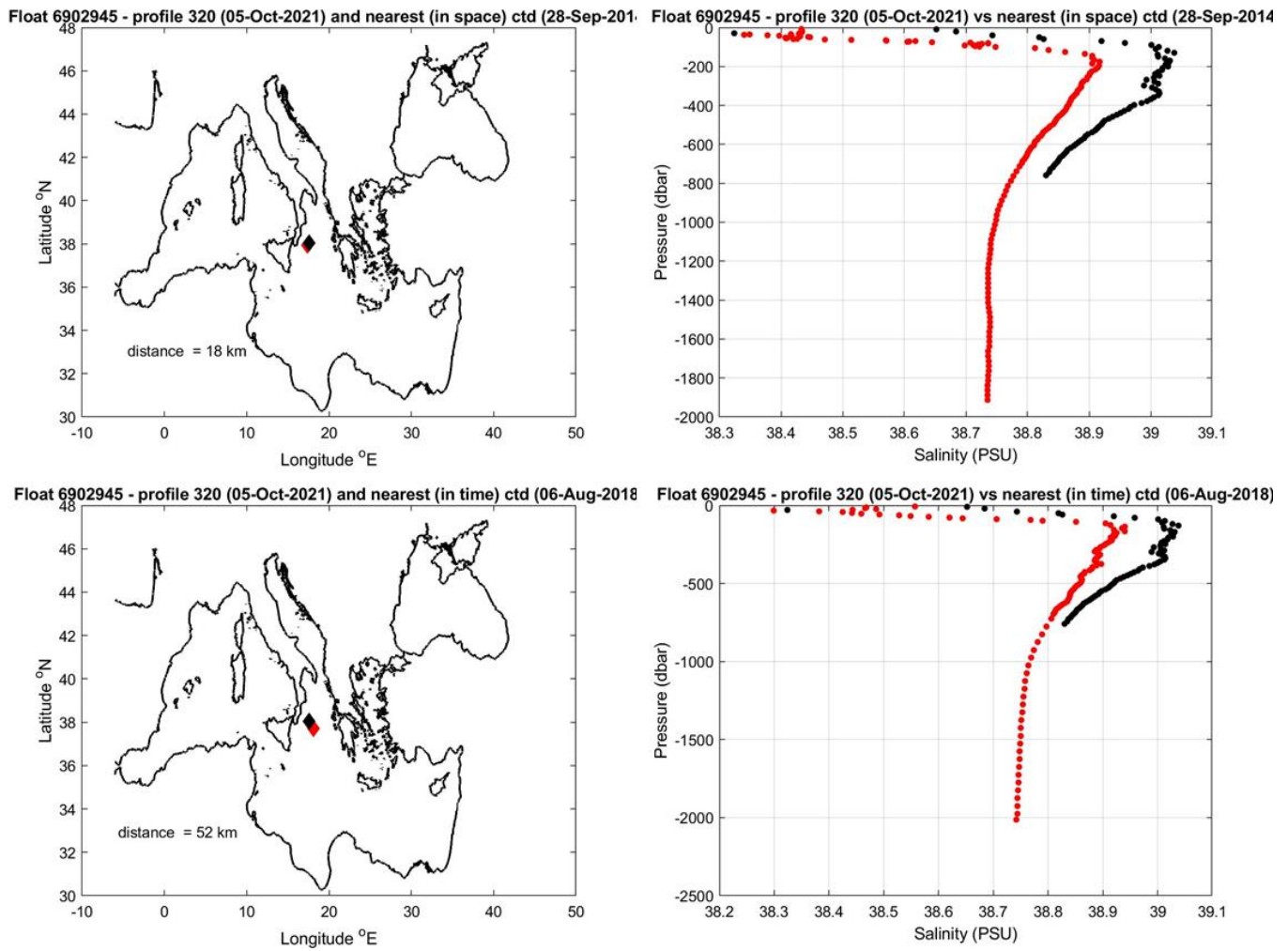
3 Correction of Salinity Data

3.1 Comparison between Argo Float and CTD Climatology

3.1.1 Configurations

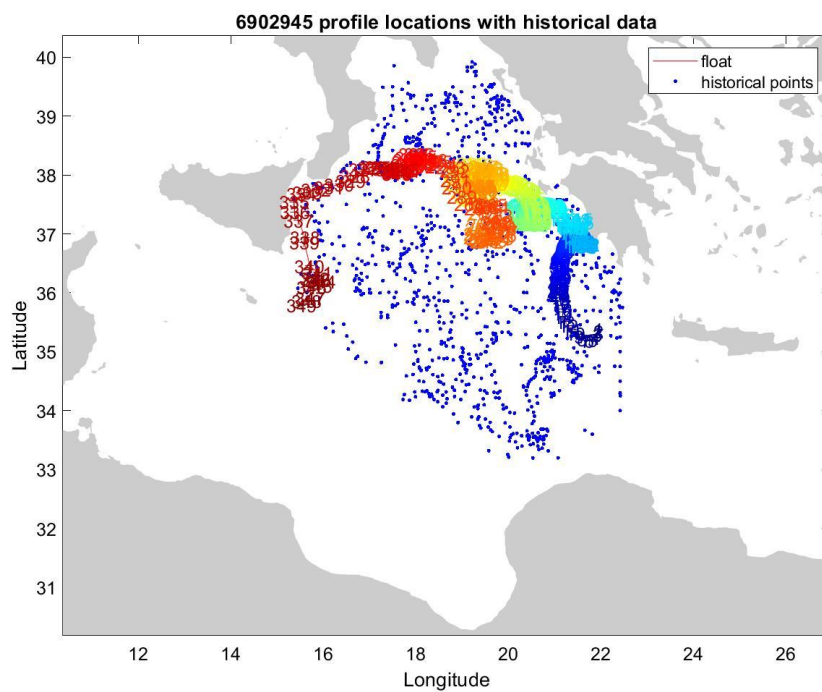| Parameters	Value
CONFIG_MAX_CASTS	300
MAP_USE_PV	1
MAP_USE_SAF	0
MAPSCALE_LONGITUDE_LARGE	4
MAPSCALE_LONGITUDE_SMALL	1.33
MAPSCALE_LATITUDE_LARGE	4
MAPSCALE_LATITUDE_SMALL	1.33
MAPSCALE_PHI_LARGE	0.5
MAPSCALE_PHI_SMALL	0.1
MAPSCALE_AGE	10
MAP_P_EXCLUDE	700
MAP_P_DELTA	250

3.1.2 Results

Figure 11: Float 6902945. Location of the float profiles (red line with colored numbers) and the reference data selected for mapping (blue dots).
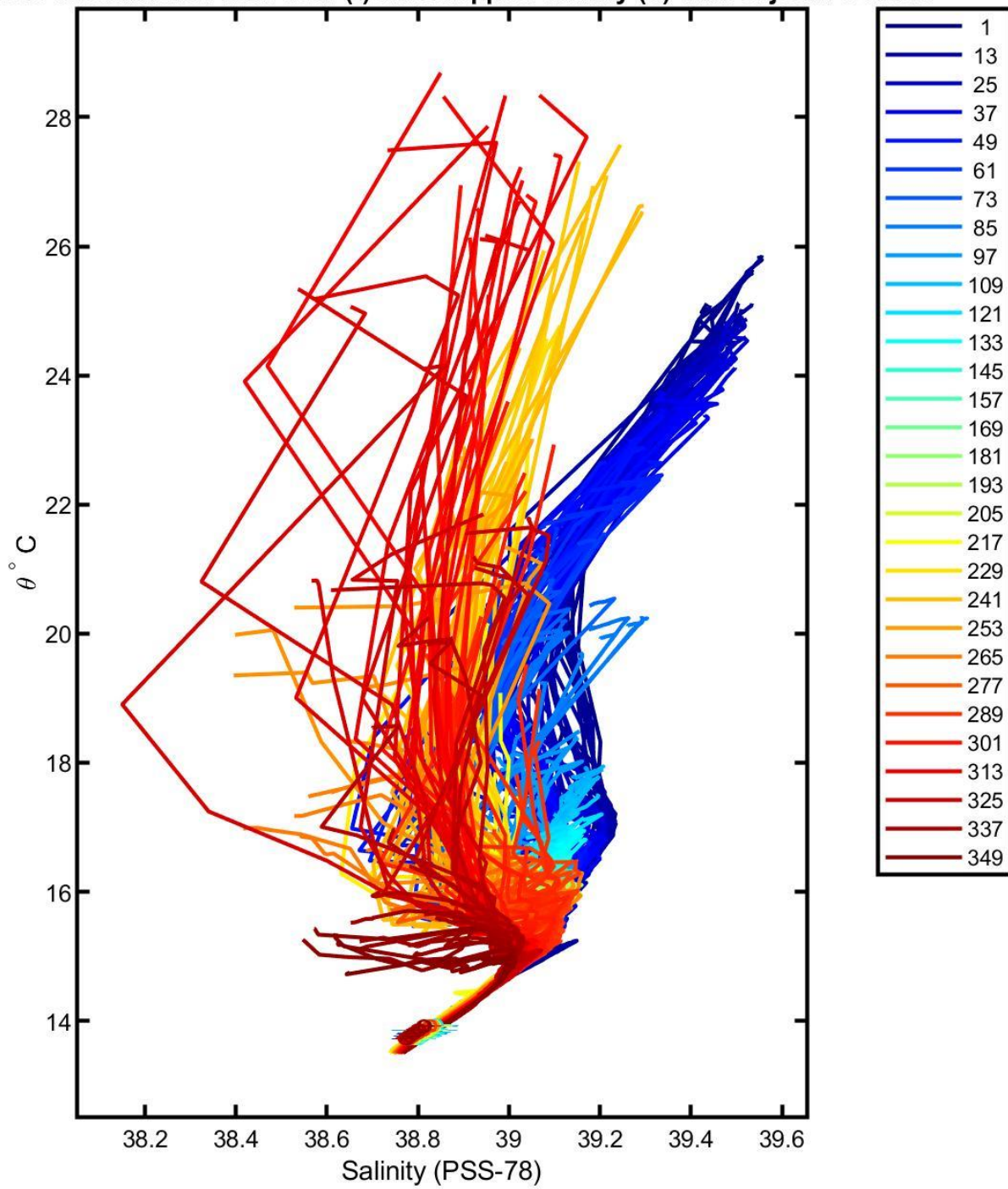
Figure 12: Float 6902945. Plot the original float salinity and the objectively estimated reference salinity at the 10 float theta levels that are used in calibration.

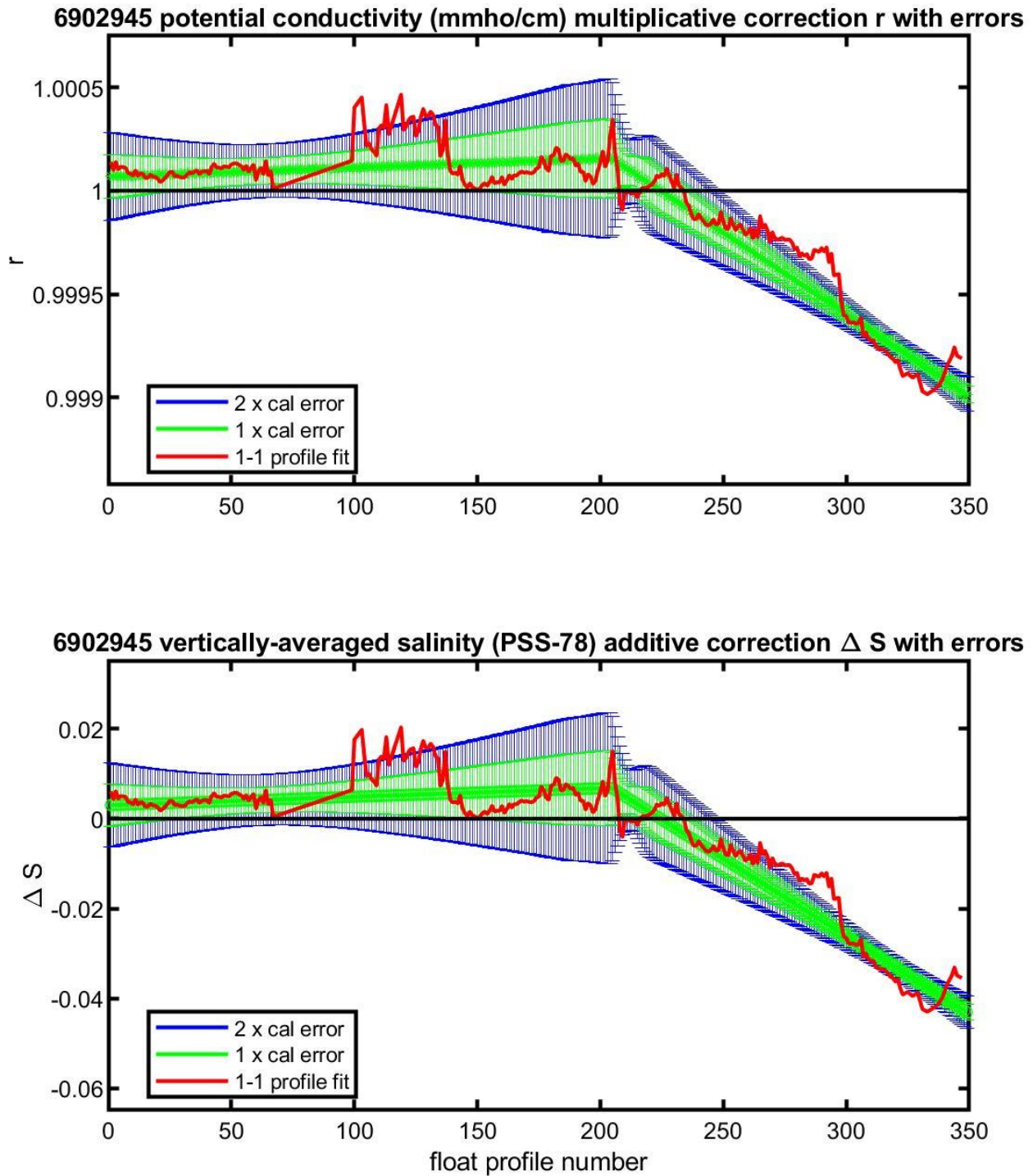**Figure 13**: Float 6902945. Evolution of the suggested adjustment with time. The top panel plots the potential conductivity multiplicative adjustment. The bottom panel plots the equivalent salinity additive adjustment. The red line denotes one-to-one profile fit that uses the vertically weighted mean of each profile. The red line can be used to check for anomalous profiles relative to the optimal fit.
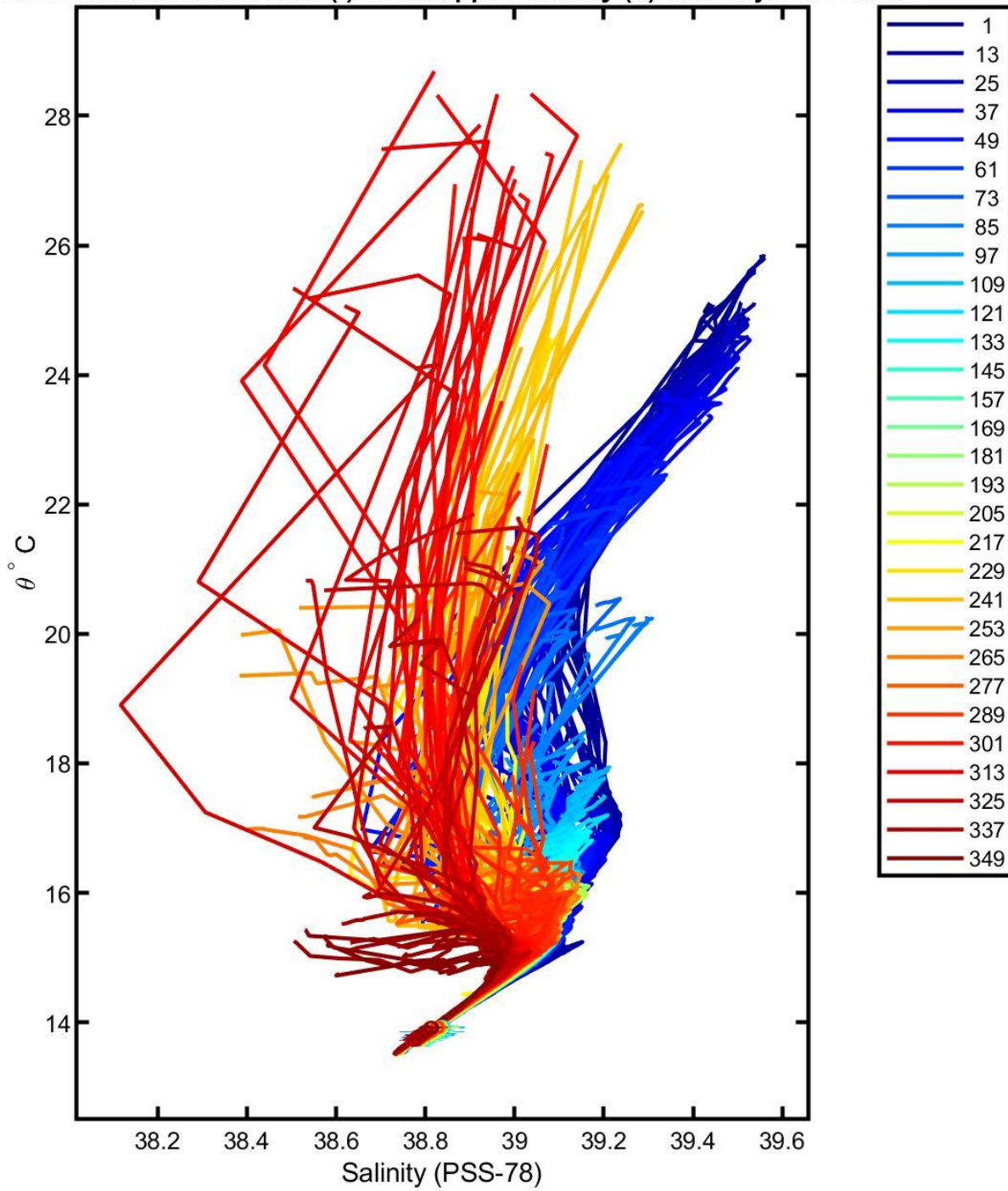
Figure 14: Float 6902945. The plot of calibrated float salinity and the objectively estimated reference salinity at the 10 float theta levels that are used in calibration.

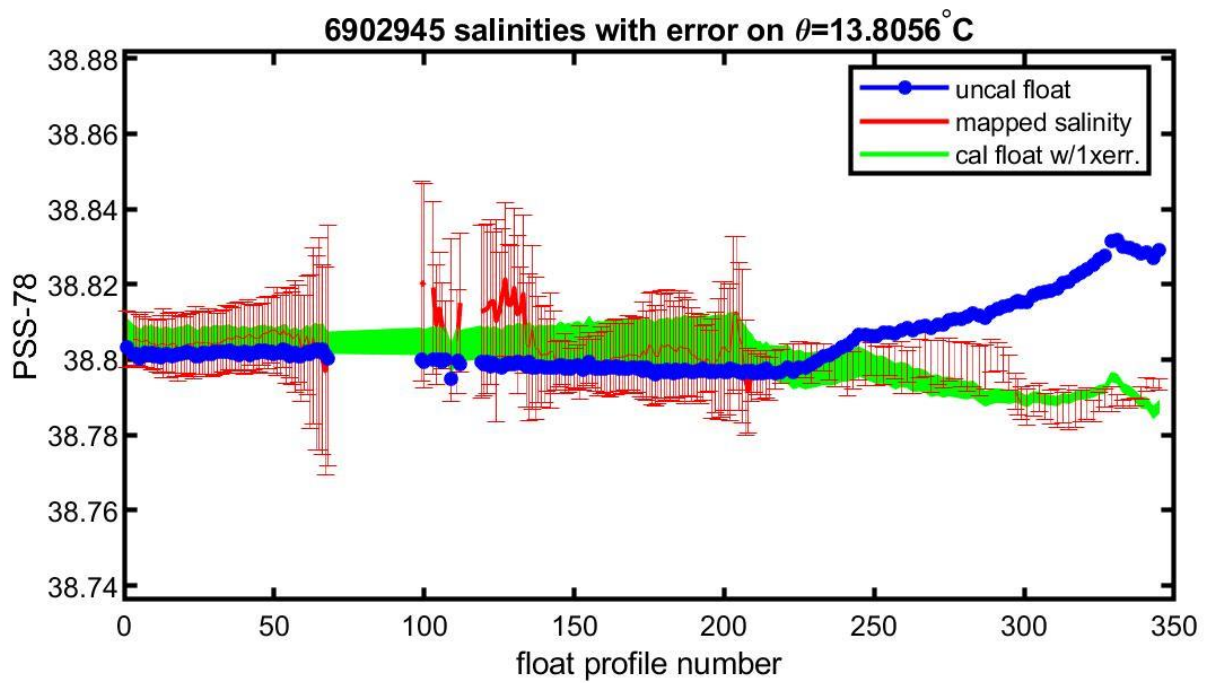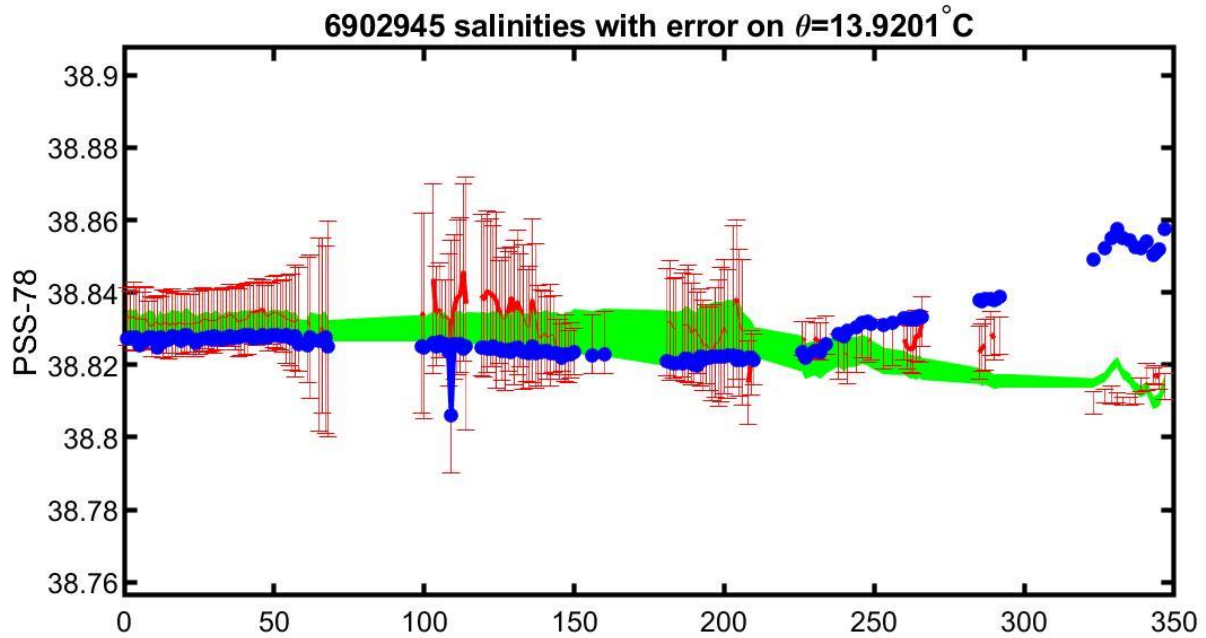**Figure 15:** Float 6902945. Plots of the evolution of salinity with time along with selected theta levels with minimum salinity variance.
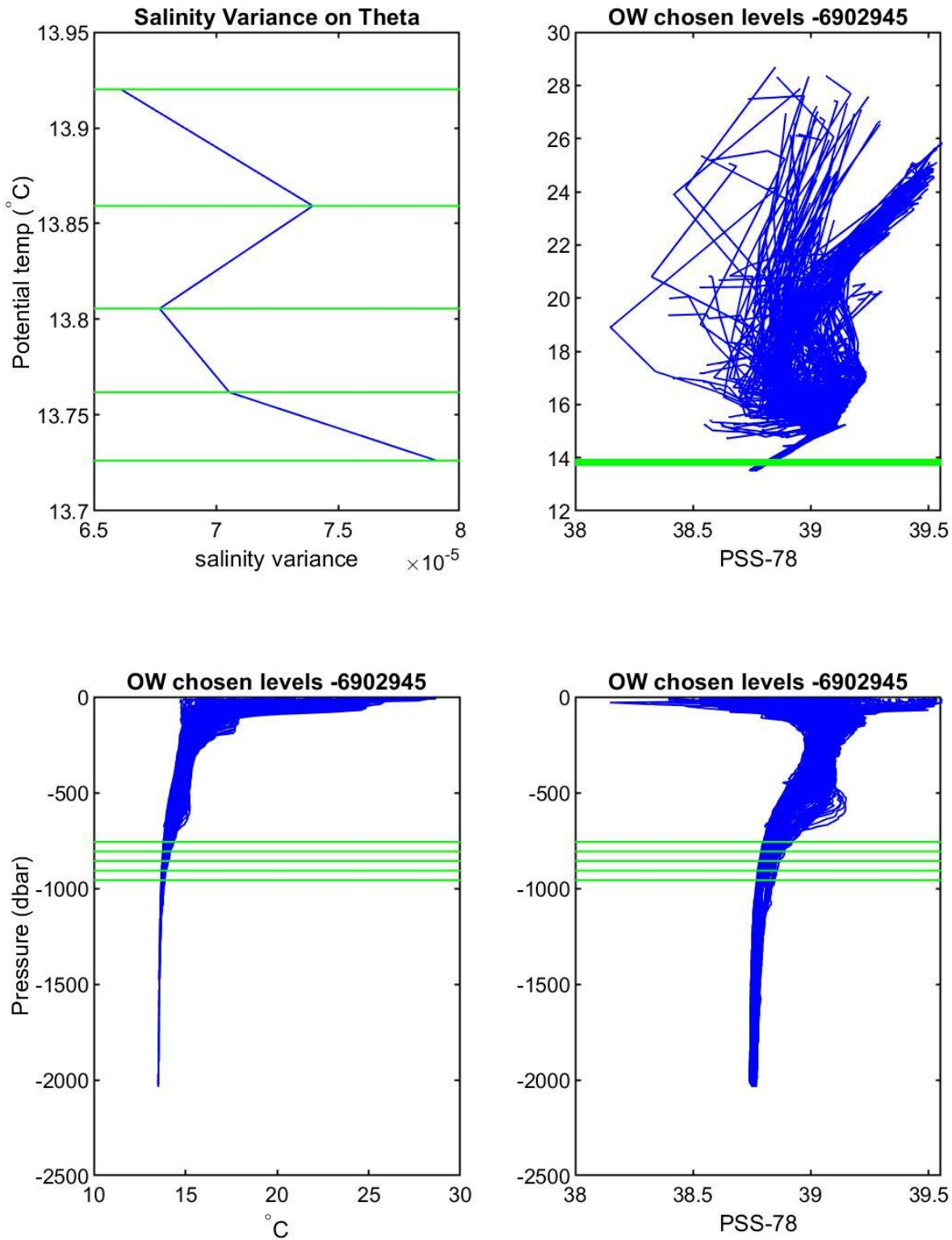
Figure 16: Float 6902945. Plots include the theta levels chosen for calibration: Top left: Salinity variance at theta levels. Top right: T/S diagram of all profiles of Argo float. Bottom left: potential temperature plotted against pressure. Bottom right: salinity plotted against pressure.

The analysis of the θ-S diagram of profile segments deeper than 700 dbar (Figure 17) shows that the OW method was run where the θ-S relationship is the tightest.

Figure 17: Float 6902945. Uncalibrated float salinity profile (black lines) and mapped historical data (red lines) in the most uniform part of the θ-S curve.

4 Summary

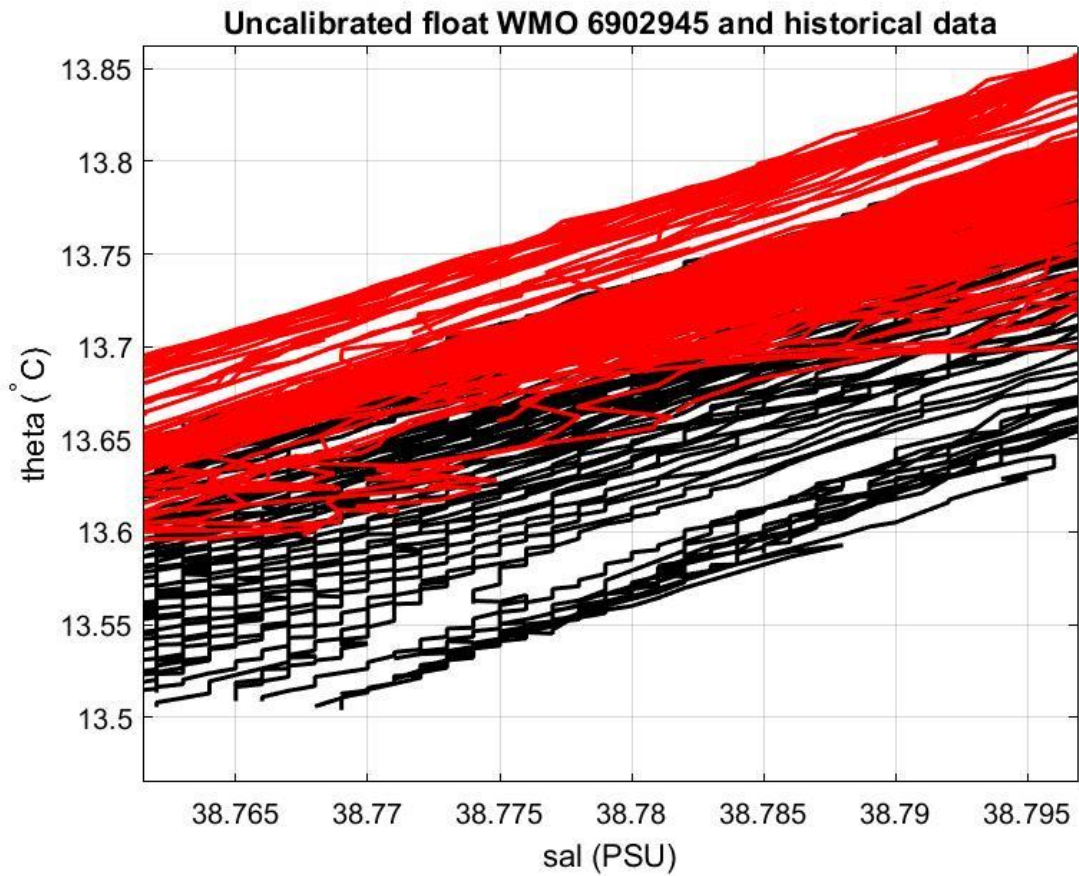Float was deployed in the Ionian sub-basin, in the Mediterranean Sea. It is still active. The most favorable water masses, which are useful for comparison with climatology is relatively stable intermediate and deep waters from around 700 m. The initial comparison between Argo float and reference data shows a potential salinity offset/drift. This float was DMQC-ed before.

The OWC analysis showed a significant salinity offset/drift. Figure 15 shows a salinity drift on selected θ levels which increases becoming significant by cycle 266. This float has some characteristics of a fast salty drifter: the correction starts from cycle 1 and float salinity data drifted salty abruptly and rapidly from cycle 266.

After several analyses, the last decision is that the salinity data of float WMO 6902945 needs a delayed mode correction for cycle from 1 to 265. QC 1 is applied. Salinity data of cycles from 266 to 349 are bad and unadjustable. QC 4 is applied.

PSAL_ADJUSTED= PSAL + ΔS from cycle 1 to 265

PSAL_ADJUSTED= PSAL from cycle 265 to 349

The quality flags applied are the following:

PSAL_ADJUSTED_QC='1' from cycle 1 to 265

PSAL_ADJUSTED_QC='4' from cycle 266 to 349

The delayed-mode files (Dfiles) have been created accordingly and sent to the Coriolis GDAC.

5 References

Cabanes, C., Thierry, V., & Lagadec, C. (2016). Improvement of bias detection in Argo float conductivity sensors and its application in the North Atlantic. Deep-Sea Research Part I: Oceanographic Research Papers, 114, 128–136. https://doi.org/10.1016/j.dsr.2016.05.007